Size fractionation and characterization of nanocolloidal particles in soils

Tang, Z. Y., Wu, L. H., Luo, Y. M., & Christie, P. (2009). Size fractionation and characterization of nanocolloidal particles in soils. Environmental Geochemistry and Health, 31(1), 1-10. DOI: 10.1007/s10653-008-9131-7

Published in:
Environmental Geochemistry and Health

Environ Geochem Health (2009) 31:1–10
DOI 10.1007/s10653-008-9131-7

ORIGINAL PAPER

Size fractionation and characterization of nanocolloidal particles in soils

Zhiyun Tang · Longhua Wu · Yongming Luo · Peter Christie

Received: 30 August 2007 / Accepted: 9 January 2008 / Published online: 5 February 2008

Abstract A protocol was developed to fractionate soil particles down to the nanocolloid scale by combining sieving, sedimentation, centrifugation, and cross-flow filtration (CFF). The validity of the method and the performance of the CFF system were tested by characterizing fractions using laser granulometry, electron microscopy, and chemical analysis. The 0.1-μm-pore-size membrane CFF system effectively retained nanocolloids (<0.1 μm) as shown by laser granulometry and observed directly by transmission electron microscopy. However, environmental scanning electron microscopy images of freeze-dried colloids were very different from their TEM counterparts, suggesting that sample preparation influenced microscopy imaging. Chemical analysis of Cu, Cd, and organic carbon in each fraction showed that the concentrations of these components increased as particle size decreased, indicating colloids and nanocolloids play an important role in retaining trace metals. Particle-size fractionation combined with chemical analysis and electron microscopy can provide insight into the nature and properties of nanocolloids in soil.

Keywords Soil particles · Nanocolloids · Cross-flow filtration · Fractionation · Laser granulometry · Electron microscopy

Z. Tang · L. Wu (✉) · Y. Luo
Key Laboratory of Soil Environment and Pollution Remediation, State Key Laboratory of Soil and Sustainable Agriculture, Institute of Soil Science, Chinese Academy of Sciences, PO Box 821, Nanjing 210008, China
e-mail: lhwu0603@yahoo.com.cn

Z. Tang
Graduate School of the Chinese Academy of Sciences, PO Box 3908, Beijing 100049, China

Z. Tang
Geological Survey of Jiangsu Province, 700 Zhujiang Road, Nanjing 210018, China

P. Christie
Agricultural and Environmental Science Department, Queen's University Belfast, Newforge Lane, Belfast BT9 5PX, UK

Introduction

Colloids, composed of particles between 1-nm and 1-μm equivalent spherical diameter, are ubiquitous in the environment. Natural colloids are mixed complexes of silicates, inorganic oxides and humic substances (Doucet et al. 2004, 2005) with a broad particle size distribution and diversity of shapes (Baalousha et al. 2006). Colloids in soil and water are involved in the adsorption, transport, and transformation of heavy metals, organic pollutants, and nutrients (Means and Wijayaratne 1982; McCarthy and Zachara 1989; Orlandini et al. 1990; Ledin et al. 1995; Lead et al. 1997, 1999; Doucet et al. 2001).

Interactions between colloids and environmental pollutants depend on particle size, shape, and surface area (Ran et al. 2000; Denaix et al. 2001). In order to understand the underlying mechanisms, it is necessary to separate colloids from the bulk sample (matrix) and then characterize them by chemical and instrumental methods. Progress in this field, however, has been hampered by the lack of efficient methods for the fractionation and characterization of natural colloids (Filella et al. 1997). Furthermore, these substances occur in low concentrations, and their suspensions are not very stable.

Traditional fractionation methods include settling, centrifugation, flocculation, and membrane filtration. The primary requirements for sampling and fractionation of colloids are reliability, lack of bias, and minimum perturbation of their native forms (Baalousha et al. 2005). A wide variety of techniques have been applied to fractionate colloids, including split-thin flow fractionation (SPLIFF) (Contado et al. 2003), flow field-flow fractionation (FIFFF) (Benedetti et al. 2002; Lyvén et al. 2003; Baalousha et al. 2005, 2006), sedimentation field-flow fractionation (SdFFF) (Ranville et al. 1999; Ran et al. 2000), and cross-flow filtration (CFF, also called tangential flow filtration (TFF)) (Guo et al. 2000; Hoffmann et al. 2000; Wilding et al. 2004; Doucet et al. 2004, 2005). Among these fractionation techniques cross-flow filtration has perhaps been the most widely used (Powell et al. 1996; Stordal et al. 1996; Benoit and Rozan 1999; Guéguen et al. 2002). CFF is a pressure-driven process in which the suspension is re-circulated parallel to the membrane. This restricts the accumulation of particles on the membrane surface, allowing large quantities of water to be processed, while membrane clogging is less of a problem than in standard filtration (Burba et al. 1998).

On the other hand, no single method has so far been shown to be adequate for the characterization of colloidal particles. This is because colloids are chemically heterogeneous as well as being diverse in size. Characterization methods involving a preliminary separation step have clear advantages since the size range and heterogeneity of each fraction are reduced, and many fractions can be collected for analysis.

The particle-size distribution and chemical properties of aquatic colloids have been the subject of numerous studies (Lead et al. 1997, 1999; Ran et al. 2000). Relatively little information, however, is available about soil colloids and their role in soils even though a substantial percentage of the soil mass is frequently composed of colloidal particles. Séquaris and Lewandowski (2003) used sedimentation and centrifugation to separate the <2-μm fraction of agricultural surface soils, but did not attempt to obtain nanocolloidal fractions. Here we develop a protocol for sequentially separating soil into nanocolloidal particle-size fractions using CFF. We also describe several analytical techniques, including laser diffraction granulometry, transmission electron microscopy (TEM), and inductively coupled plasma-atomic emission spectrometry (ICP-AES) for characterizing the size, shape, and chemical composition of the separated fractions.

Materials and methods

Sampling and fractionation

Samples of three Chinese soils were collected from the top 15 cm of the profiles at Dexing in Jiangxi province (DX-9), Fuyang in Zhejiang province (FY-1), and Jiuhua in Jiangsu province (JH-4). They are an alumi-orthic acrisol, fluvio-marine yellow soil, and typic ferri-udic argosol, respectively, according to the Chinese Soil Taxonomy System (Cooperative Research Group on Chinese Soil Taxonomy 2001). After air-drying and removal of stones and visible plant materials, the samples were passed through a 250-μm mesh nylon sieve. Some basic chemical properties of the three soil samples are listed in Table 1.

The separation of soil particles was performed using the following protocol. All procedures were conducted in duplicate, and the protocol was completed within 2 days.

Table 1 Basic physicochemical properties of selected soil samples

Soil sample	pH (in water)	Org. C, g kg^{-1}	CEC, cmol(+) kg^{-1}
JH-4	7.34	17.0	19.2
FY-1	7.72	19.9	13.2
DX-9	4.34	12.2	11.9

(1) The 50–250-μm fine sand. The air-dried soils were ground and passed through a 60-mesh nylon sieve, then 50 g (oven dry weight) of the sieved soil was added to a measuring cylinder containing 1 l deionized water and left overnight before ultrasonic dispersion for 10 min at 25°C. No chemical dispersing agent was added to avoid the decay of soil aggregates. The suspension was slowly poured through a 300-mesh nylon sieve (50 μm) that was carefully washed with deionized water. Particles remaining on the sieve were collected and dried at 60°C. This procedure collected the 50–250-μm fine sand particles.

(2) The 5–50 μm silt. The suspension containing particles that passed through a 300-mesh nylon sieve was transferred to a 3-l glass beaker. Deionized water was added until the volume of the suspension was 3 l, mixed thoroughly, and left to sediment for 1 h and 14 min (at 20°C ambient temperature). The upper layer of liquid (0–10 cm from the surface) was then siphoned off. The sedimentation time was calculated according to Stokes' Law. This procedure was repeated 15–20 times until the upper layer liquid appeared clear and showed no Tyndall effect. All the siphoned liquid was combined for further seperation at step (3), and the sediment was collected and dried at 60°C. This process separated the 5–50 μm slit particles.

(3) The 1–5-μm fine silt. All the siphoned liquid from Step (2) was collected, and 200-ml aliquots were placed in 300-ml centrifuge tubes and centrifuged (Model TDL-5, Anting Scientific Instrument Company, Shanghai, China) at 1,500 rpm (RCF 433 g) for 5 min. The supernatant was carefully transferred to a clean plastic bucket for further separation at step (4). All the centrifuged residues were recovered, combined, and freeze dried. This process separated the 1–5-μm fine silt particles in the soil.

Stokes' law was used to calculate settling and centrifugation times assuming a particle density of 2.5 g cm^{-3}. Centrifuge time was calculated by the formula $t = (\eta \lg(R_2/R_1))/(3.81N^2r^2\Delta d^2)$, where R_1 is the distance from the surface of the liquid in the centrifuge tube to the center of the axis of the centrifuge; R_2 is distance from the particles in the centrifuge tube to the center of the axis of the centrifuge; N is the centrifuge speed (rev s^{-1}); r is the radius of the particles in the liquid in the centrifuge tube; Δd is the difference in density between the particles and water, which we set at 1.65 g cm^3; η is the water viscosity coefficient (0.01005 g cm^{-1} s^{-1} at 20°C). The relative centrifugation force (RCF, g) = $11.2 \times r \times (\text{rpm}/1000)^2$, where r is the distance from the bottom of the centrifuge tube to the center of the axis of the centrifuge, and rpm is the centrifuge speed (rev min^{-1}).

(4) The 0.1–1-μm colloid fraction. Each 200 ml of the supernatant from step (3) was placed in a 300-ml centrifuge tube and centrifuged at 4,500 rpm (RCF 3,900 g) for 54 min. The supernatant was carefully retained for further separation at step (5). All the residues were combined and dried at 60°C. This process separated the 0.1–1 μm colloidal fraction.

The centrifuge method was used here instead of sedimentation to save time and to minimize changes in soil properties within a short separation time.

(5) The <0.1-μm nanocolloid fraction. The <0.1-μm nanocolloidal fractions were present in the supernatant from the colloidal fraction at step (4). About 10–12 l of supernatant was collected from step (4), filtered through a 2-μm regenerated cellulose acetate membrane, and then passed through a Cross-Flow Filtration (CFF) device (Model A, Tianjin Polytechnic University Motian Group, Tianjin, China) equipped with a hollow fiber polyvinylidene fluoride (PVDF) cassette filter with a diameter of 0.1 μm and a surface area of 0.2 m^2, giving a permeate (material that passed through the CFF membrane) and a retentate (nanocolloids retained by the membrane). Before and after each fractionation, the membranes were thoroughly cleaned, and their permeability was carefully tested according to the manufacturer's instructions. The CFF process was assumed to be complete when the volume of the retentate was about 300 ml. Any residue from the system was backwashed three times with deionized water to wash out the nanocolloids adhering to the PVDF tube, and the retentate and washings were transferred to a 1-l polyethylene bottle.

The soil samples were separated into five size fractions by the above combination of wet sieving (250–50 μm), gravity sedimentation (50–5 μm), and centrifugation (1–5 μm) and CFF methods (0.1–1 μm).

Size distribution analysis

Laser diffraction granulometry

Upon completion of each separation step, the fraction was transferred to a polyethylene bottle, refrigerated, and stored at 4°C in the dark. Size distributions of

all five fractions were determined before freeze-drying using a laser diffraction granulometer (LS230, Beckman Coulter), equipped with a variable-speed fluid module covering the range 0.4–2,000 μm. The size measurement is based on the relationship between the light intensity pattern (diffracted by a laser light of wavelength 750 nm into 126 photodiode detectors) and particle diameter. By using a single frequency polarized light beam scattered onto banks of an additional six detectors, sub-micron particles down to 0.04 μm can be detected. Integration of data from the two systems allowed the size range to be extended to 0.04–2,000 μm. This was particularly useful for analyzing clay-rich soils. The size was calculated in terms of volume percent distribution on the basis of the Fraunhofer approximation. A more detailed description of the methodology has been given by Pye and Blott (2004). Determinations were performed on aqueous soil suspensions.

Electron microscopy imaging

Transmission electron microscopy (TEM) and environmental scanning electron microscopy (ESEM) were combined to examine the size and shape of nanocolloid particles. TEM was carried out using a JEL-1230 (JEOL) instrument. Samples for TEM were prepared by immersing a TEM grid (300-mesh Cu Holey carbon coated) in the nanocolloid suspension and absorbing the water into a filter paper. High-vacuum ESEM experiments were carried out with a field emission scanning electron microscope (Philips XL30 ESEM) operating at an acceleration voltage of 20 kV.

Chemical analysis

Concentrations of Si, Fe, Al, Mn, Ca, Mg, K, and Na in the CFF permeates and nanocolloids stored at 4°C were determined simultaneously by inductively coupled plasma-atomic emission spectrometry (ICP-AES, Intrepid II, Thermo). Leachate passing through a slow-speed filter paper (1–3 μm of aperture) can be used directly for determination of elemental contents. The nanocolloids we collected were centrifuged to nanosize and again passed through a 2-μm membrane to make them suitable for determination of elemental contents. The flame temperature was about 6,000–7,000 K, high enough for atomization of Fe, Al, and Si. We therefore determined the Fe, Al, and Si concentrations of the nanocolloids directly. This also avoided the precipitation of Si when the samples were digested using the *aqua regia* method.

After laser granulometry and ICP-AES determinations, each fraction was freeze-dried and homogenized. The concentrations of Cu and Cd in all five size fractions was determined by ICP-MS (X7, Thermo), and total organic carbon (TOC) was measured by dichromate oxidation (Xiong 1985).

Results and discussion

CFF performance

Table 2 shows the elemental composition of the nanocolloids and their respective permeates from the three soils as determined by ICP-AES. The concentrations of Al, Fe, and Mn in permeates were close to the detection limits. Since these elements are the major components of soil colloids, this finding indicates that very little, if any, inorganic nanocolloidal material passed through the 0.1-μm pore-size membrane. Membrane filtration is a very complex process, involving many critical factors (mechanisms). Several studies have made efforts to find out the effects. A very important mechanism is the electrical double-layer interaction between membrane and dispersed particles (Bowen et al. 1999). Another is the nano-filtration mechanism (Bacchin et al. 1996). The work by Doucet et al. (2004) showed that CFF fractionation involves other factors besides size. While permeates were essentially free of particles, retentates were substantially rich in small colloids (50 nm). Our electron microscope work showed that retentates were nanoparticles (see below). Although nominal membrane pore sizes are not accurate indicators of particle size, CFF is a useful method for the fractionation and concentration of the soil suspension following centrifugation. CFF also allows up to 10 l of filtered suspensions to be concentrated to 1 l within 1 h.

Granulometric size distribution

Figure 1 shows the size distributions of the five soil fractions of the DX-9 soil as determined by laser

Table 2 Elemental compositions of nanocolloids and their permeates

Soil	Fraction	Molar ratio[a]		Al[b]	Fe[b]	Mn[b]	Si	K	Na	Mg	Ca
		Al/Si	Fe/Si								
JH-4	Colloids	0.593	0.251	10.4 ± 0.2	9.08 ± 0.12	0.05 ± 0.01	18.8 ± 0.2	1.38 ± 0.10	0.36 ± 0. 03	0.95 ± 0.02	3.95 ± 0.25
	Permeates			0.005	0.005	0.005	0.61 ± 0.10	0.27 ± 0.05	0.19 ± 0.02	0.07 ± 0.01	0.86 ± 0.05
FY-1	Colloids	0.682	0.186	3.05 ± 0.11	1.72 ± 0.08	0.03 ± 0.01	5.25 ± 0.15	0.41 ± 0.03	0.39 ± 0.03	0.38 ± 0.02	10.4 ± 0.1
	Permeates			0.005	0.005	0.005	0.60 ± 0.09	0.05 ± 0.01	0.11 ± 0.02	0.19 ± 0.01	8.33 ± 0.08
DX-9	Colloids	0.931	0.529	3.07 ± 0.09	3.61 ± 0.10	0.16 ± 0.01	3.62 ± 0.11	0.68 ± 0.03	0.16 ± 0.03	0.14 ± 0.01	0.50 ± 0.04
	Permeates			0.005	0.005	0.005	0.19 ± 0.05	0.35 ± 0.04	0.17 ± 0.03	0.04 ± 0.01	0.49 ± 0.04

Units: mg l^{-1}

[a] Molar ratio = mole of Al or Fe/(mole of colloid Si−mole of permeates Si)

[b] The detection limit of Al, Fe and Mn by ICP-AES was 0.005 mg l^{-1}

granulometry. The fine sand fraction (50–250 μm, Fig. 1a) had a unimodal, symmetrical, and well-defined size distribution with a mean diameter of 109 μm, indicating that wet sieving was effective in separating sand. The silt fraction (5–50 μm, Fig. 1b) had a mean diameter of 11.1 μm and showed a bimodal distribution with the primary mode being centered at a diameter of 16.4 μm, while the secondary distribution had a mode diameter of 1.0 μm. This effect may be attributed to the presence of a small amount of water-dispersible soil aggregates in the silt fraction, which otherwise had a well-defined size distribution. Likewise, the fine silt fraction (1–5 μm) had a well-defined, unimodal size distribution with a mean diameter of 3.38 μm (Fig. 1c). The small tail in the colloidal (clay) fraction suggests that some clay-size particles were carried into the fine silt fraction. The colloid fraction (0.1–1 μm, Fig. 1d) showed three separate size modes, with the principal one having a well-defined, narrow size distribution with a mean diameter of 0.635 μm. The appearance of larger particles (ca. 2 μm) was probably due to disturbance by spiralling water during centrifugation. The nanocolloid fraction (<0.1 μm, Fig. 1e) had a size distribution with four separate size modes. The size distributions of all fractions of soils JH-4 and FY-1 were the same as those of DX-9. This suggests that strong disturbance by water during the fractionation and centrifugation may have occurred as the concentration of nanocolloids was low.

Figure 2a shows that large particles (ca. 2 μm) were removed when the supernatants (about 10 l) from the colloid fraction of soil DX-9 were filtered through a 2-μm membrane (regenerated cellulose acetate) and concentrated using the CFF system. Sequential centrifugation of the filtered colloid suspension at above designated conditions yielded more purified nanocolloids (Fig. 2b). Statistical analysis revealed that 85.9% of the volume was occupied by particles <0.1 μm, with larger particles (ca. 0.2 μm) making up the rest (14.1%). This fraction had a bimodal size distribution with a mean diameter of 0.076 μm.

Since size calculations were based on the assumption that the soil particles were spherical and had uniform composition and density, the volume of flat particles in each fraction may have been overestimated, while that of elongated or very angular particles may have been underestimated. Moreover, the low-density particles in the fractions would have had a relatively large size distribution.

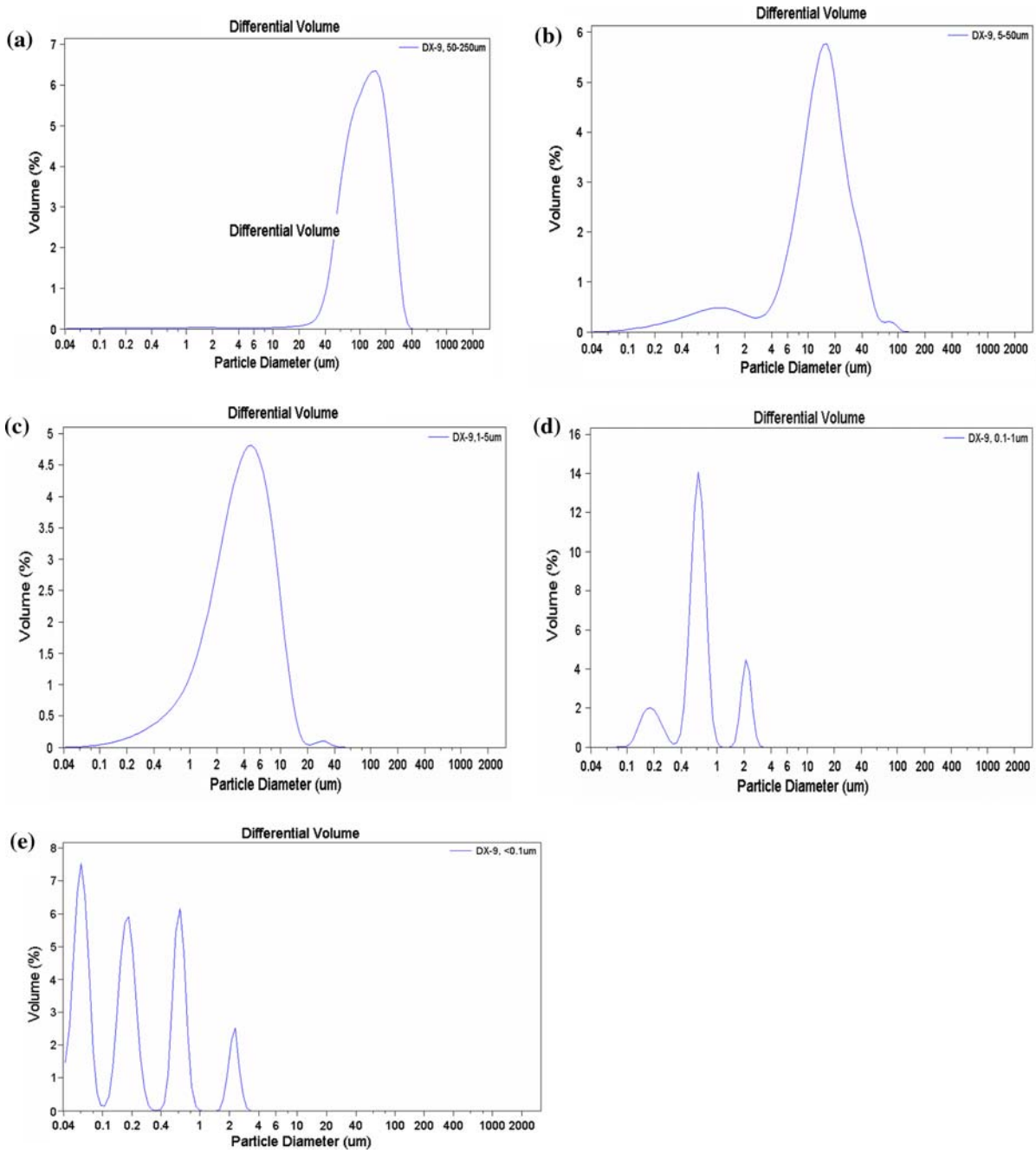

Fig. 1 Soil particle size distribution of soil DX-9: (**a**) fine sand (250–50 μm), (**b**) very fine sand (50–5 μm), (**c**) silt (5–1 μm), (**d**) colloids (1–0.10 μm), and (**e**) nanocolloids (<0.10 μm)

Electron microscope imaging of colloidal fractions

Both TEM and SEM have often been used to visualise the size and shape of aquatic colloids and other particles (Wilkinson et al. 1999; Redwood et al. 2005). Here, the purified nanocolloid fractions were analyzed by TEM to validate laser granulometry measurements and assess the capability of CFF to retain nanocolloidal particles. The TEM images of

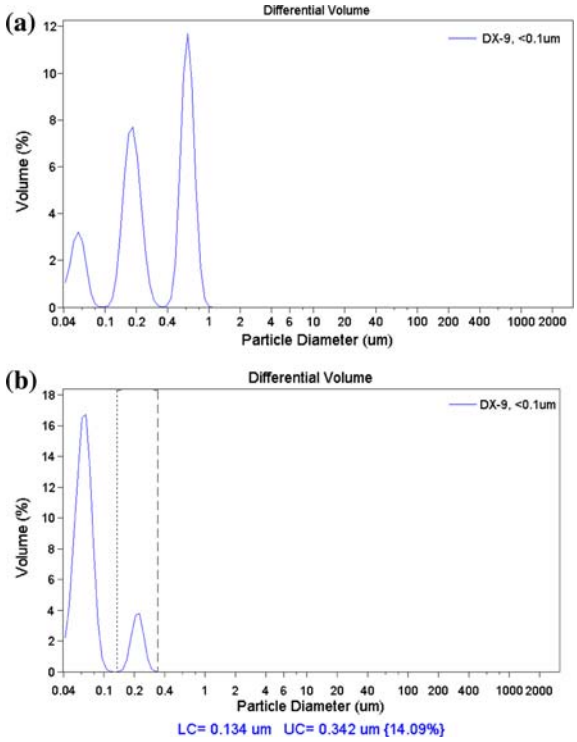

Fig. 2 Size distribution of purified nanocolloids: (**a**) filtered through a 2-μm membrane and (**b**) suspension of (**a**) purified by centrifugation

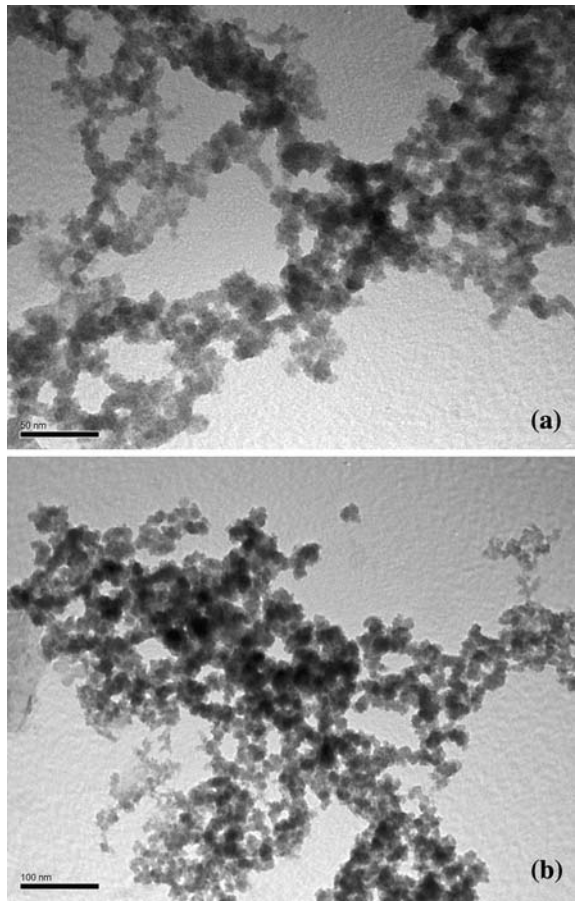

Fig. 3 TEM observation of soil DX-9 nanocolloids at two levels of magnification: (**a**) scale bar 50 nm and (**b**) scale bar 100 nm

nanocolloids from the DX-9 soil (Fig. 3) show that the dominant materials were almost uniform in size, with a diameter of about 20 nm, suggesting that the CFF system could effectively retain particles smaller than the nominal pore size. Similar results were observed in the TEM examination of the JH-4 and FY-1 nanocolloids and have been reported from other studies (Doucet et al. 2005).

On the other hand, the ESEM images of freeze-dried nanocolloids from all three soils showed relatively large, flat and smooth particles (Fig. 4). It seems that different sample preparations may have led to the different ESEM and TEM results. One explanation is colloid surface coverage by a film composed of small organic macromolecules that had flattened following drying (Doucet et al. 2004) and were presumably derived from the sample preparation technique due to the potential redistribution or self-assembly of particulate components under high vacuum conditions (Whitesides and Grzybowski 2002).

Chemical components of nanocolloids

Table 2 shows the concentrations of different elements in the nanocolloid suspensions and permeates from the three soils as determined by ICP-AES. Changes in clay minerals (Table 2) were more clearly seen by elemental mole ratio by calculating the Al/Si and Fe/Si molar ratios. One explanation for the observed trends in these ratios is that the DX-9 colloid fraction was possibly dominated by iron-oxide minerals (Fe/Si = 0.529) and 1:1 clay minerals (Al/Si = 0.931), such as kaolinite, which contain only Al, Si, O, and H, whereas the colloids of soils FY-1 and JH-4 contained more complex clay minerals, such as illite and smectite, having Fe, Mg, and other elements present in the clay structure. The Fe/Si ratio of the nanocolloid fraction showed that iron in soil DX-9 was more likely independent on the

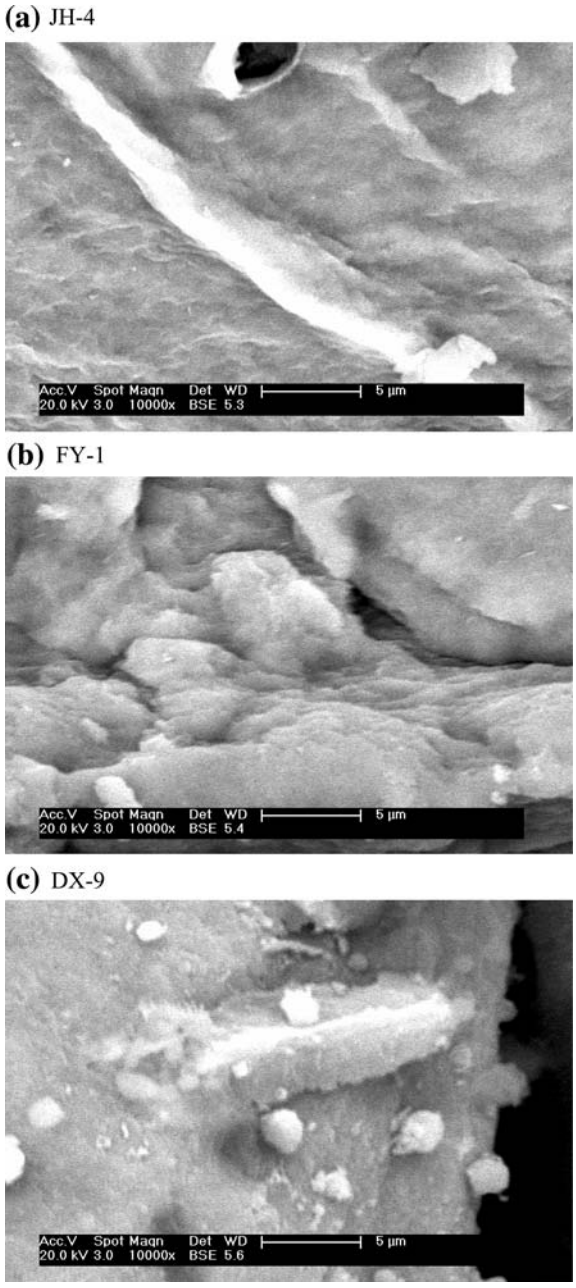

Fig. 4 ESEM images of nanocolloids of soils (**a**) JH-4, (**b**) FY-1, and (**c**) DX-9

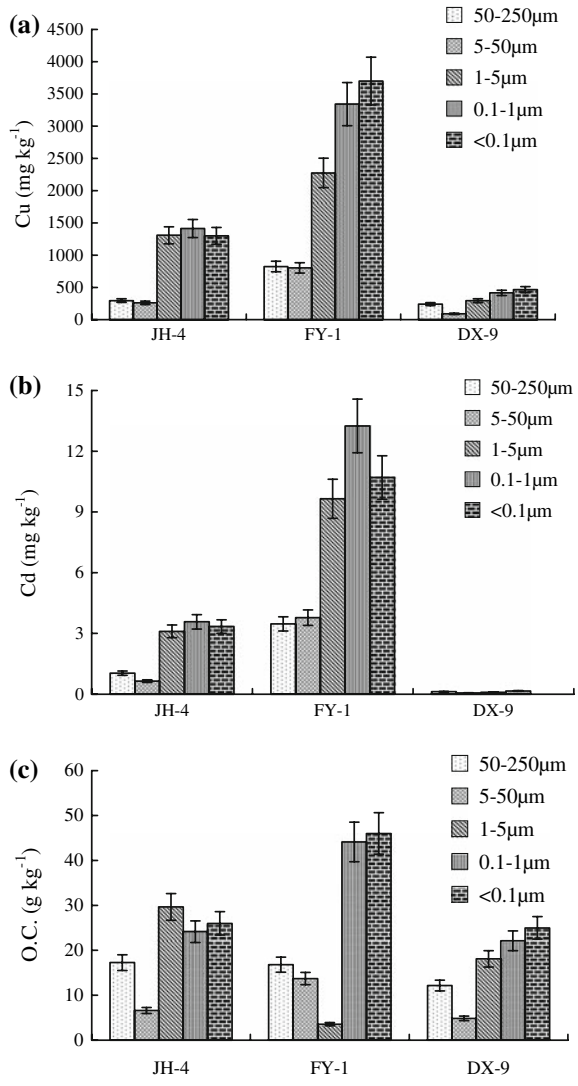

Fig. 5 Copper, Cd, and organic carbon contents in each fraction

colloidal fraction. However, we could not use X-ray diffraction to identify the nature of the minerals in the nanocolloid fractions of the soils because of the low concentrations present.

Figure 5 shows that the concentrations of Cu, Cd, and organic carbon in the five fractions increased with decreasing particle size. Figure 6 shows that the concentrations of Cu and Cd in the soil fractions are highly correlated with their respective OC content. This finding suggests that Cu is complexed with organic matter (Wen et al. 1999). The high affinity of Cd for organic ligands, however, is inconsistent with the results from other studies (Zhou and Wangersky 1989).

Conclusions

Sieving, sedimentation, and centrifugation coupled with cross-flow filtration enable soils to be

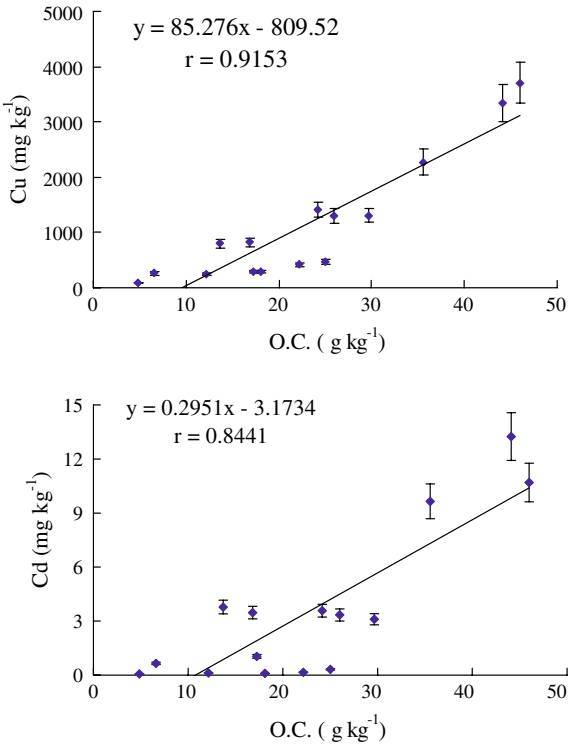

Fig. 6 Relationship between Cu, Cd, and organic C in each fraction of three soils ($n = 15$)

sequentially fractionated down to the nanocolloid level based on Stokes' law. Laser granulometry and electron microscopy show that the nominal pore size of the membrane used in the CFF system is not an accurate indicator of particle size in separated fractions. The diameter of particles retained by the (polyvinylidene fluoride) membrane is smaller than the indicated pore size.

Laser granulometry is a convenient method for monitoring particle size distribution. Environmental scanning electron microscopy (ESEM) of colloids may introduce artifacts due to sample preparation techniques. However, the combined use of ESEM and transmission electron microscopy (TEM) provides insight into soil nanocolloid distributions.

The concentrations of Cu, Cd, and organic carbon varied among the fractions, but tended to increase as particle size decreased. The concentrations of Cu and Cd are highly correlated with the organic C content, suggesting that finely divided soil particles may play an important role in environmental processes.

The partitioning of pollutants into colloids is important in determining the fate and transport of contaminants in the environment. Since these processes are dependent on colloid size (surface area), surface chemistry, and mineralogy, the chemical analysis of nanocolloids, together with their size and shape, will provide important information to further our understanding of the behavior of environmental pollutants.

Acknowledgements We thank the National Natural Science Foundation of China (project 20477048) and the Major State Basic Research and Development Program of the People's Republic of China (project 2005CB121104) for financial support.

References

Baalousha, M., Kammer, F. V. D., Motelica-Heino, M., & Le Coustumer, P. (2005). Natural sample fractionation by FIFFF–MALLS–TEM: Sample stabilization, preparation, pre-concentration and fractionation. *Journal of Chromatography A, 1093*, 156–166.

Baalousha, M., Kammer, F. V. D., Motelica-Heino, M., Hilal, H. S., & Le Coustumer, P. (2006). Size fractionation and characterization of natural colloids by flow-field flow fractionation coupled to multi-angle laser light scattering. *Journal of Chromatography A, 1104*, 272–281.

Bacchin, P., Aimar, P., & Sanchez, V. (1996). Influence of surface interaction on transfer during colloid ultrafiltration. *Journal of Membrane Science, 115*, 49–63.

Benedetti, M., Ranville, J. F., Ponthieu, M., & Pinheiro, J. P. (2002). Field-flow fractionation characterization and binding properties of particulate and colloidal organic matter from the Rio Amazon and Rio Negro. *Organic Geochemistry, 33*, 269–279.

Benoit, G., & Rozan, T. F. (1999). The influence of size distribution on the particle concentration effect and trace metal partitioning in rivers. *Geochimica et Cosmochimica Acta, 63*, 113–127.

Bowen, W. R., Hilal, N., Jain, M., Lovitt, R. W., Sharif, A. O., & Wright, C. J. (1999). The effects of electrostatic interactions on the rejection of colloids by membrane pores: Visualisation and quantification. *Chemical Engineering Science, 54*, 369–375.

Burba, P., Aster, B., Nifant'eva, T., Shkinev, V., & Spivakov, B. Y. (1998). Membrane filtration studies of aquatic humic substances and their metal species: A concise overview Part 1. Analytical fractionation by means of sequential-stage ultrafiltration. *Talanta, 45*, 977–988.

Contado, C., Blo, G., Conato, C., Dondi, F., & Beckett, R. (2003). Experimental approaches for size-based metal speciation in rivers. *Journal of Environmental Monitoring, 5*, 845–851.

Cooperative Research Group on Chinese Soil Taxonomy (2001). *Chinese soil taxonomy*. Beijing: Science Press.

Denaix, L., Semlali, R. M., & Douay, F. (2001). Dissolved and colloidal transport of Cd, Pb, and Zn in a silt loam soil affected by atmospheric industrial deposition. *Environmental Pollution, 114*, 29–38.

Doucet, F. J., Maguire, L., & Lead, J. R. (2004). Size fractionation of aquatic colloids and particles by cross-flow filtration: Analysis by scanning electron and atomic force microscopy. *Analytica Chimica Acta, 522*, 59–71.

Doucet, F. J., Maguire, L., & Lead, J. R. (2005). Assessment of cross-flow filtration for the size fractionation of freshwater colloids and particles. *Talanta, 67*, 144–154.

Doucet, F. J., Schneider, C., Bones, S. J., Kretchmer, A., Moss, I., Tekely, P., & Exley, C. (2001). The formation of hydroxyaluminosilicates of geochemical and biological significance. *Geochimica et Cosmochimica Acta, 15*, 2461–2467.

Filella, M., Zhang, J. W., Newman, M. E., & Buffle, J. (1997). Analytical applications of photon correlation spectroscopy for size distribution measurements of natural colloidal suspensions: Capabilities and limitations. *Colloids and Surfaces A: Physicochemical and Engineering Aspects, 120*, 27–46.

Guéguen, C., Belin, C., & Dominik, J. (2002). Organic colloid separation in contrasting aquatic environments with tangential flow filtration. *Water Research, 36*, 1677–1684.

Guo, L. D., Santschi, P. H., & Warnken, K. W. (2000). Trace metal composition of colloidal organic material in marine environments. *Marine Chemistry, 70*, 257–275.

Hoffmann, S. R., Shafer, M. M., Babiarz, C. L., & Armstrong, D. E. (2000). A critical evaluation of tangential flow ultrafiltration for trace metal studies in freshwater systems. 1. Organic carbon. *Environmental Science and Technology, 34*, 3420–3427.

Lead, J. R., Davison, W., Hamilton-Taylor, J., & Buffle, J. (1997). Characterizing colloidal material in natural waters. *Aquatic Geochemistry, 3*, 213–232.

Lead, J. R., Hamilton-Taylor, J., Davison, W., & Harper, M. (1999). Trace metal sorption by natural particles and coarse colloids. *Geochimica et Cosmochimica Acta, 63*, 1661–1670.

Ledin, A., Karlsson, S., Duker, A., & Allard, B. (1995). Characterization of the submicrometer phase in surface waters: A review. *Analyst, 120*, 603–608.

Lyvén, B., Hassellöv, M., Turner, D. R., Haraldsson, C., & Andersson, K. (2003). Competition between iron- and carbon-based colloidal carriers for trace metals in a freshwater assessed using flow field-flow fractionation coupled to ICPMS. *Geochimica et Cosmochimica Acta, 67*, 3791–3802.

McCarthy, J. F., & Zachara, J. M. (1989). Subsurface transport of contaminants: Mobile colloids in the subsurface environment may alter the transport of contaminants. *Environmental Science and Technology, 23*, 496–502.

Means, J. C., & Wijayaratne, R. (1982). Role of natural colloids in the transport of hydrophobic pollutants. *Science, 215*, 968–970.

Orlandini, K. A., Penrose, W. R., Harvey, B. R., Lovett, M. B., & Findlay, M. W. (1990). Colloidal behavior of actinides in an oligotrophic lake. *Environmental Science and Technology, 24*, 706–712.

Powell, R. T., Landing, W. M., & Bauer, J. E. (1996). Colloidal trace metals, organic carbon and nitrogen in a southeastern US estuary. *Marine Chemistry, 55*, 165–176.

Pye, K., & Blott, S. J. (2004). Particle size analysis of sediments, soils and related particulate materials for forensic purposes using laser granulometry. *Forensic Science International, 144*, 19–27.

Ran, Y., Fu, J. M., Sheng, G. Y., Beckett, R., & Hart, B. T. (2000). Fractionation and composition of colloidal and suspended particulate materials in rivers. *Chemosphere, 41*, 33–43.

Ranville, J. F., Chittleborough, D. J., Shanks, F., Morrison, R. J. S., Harris, T., Doss, F., & Beckett, R. (1999). Development of sedimentation field-flow fractionation-inductively coupled plasma mass spectrometry for the characterization of environmental colloids. *Analytica Chimica Acta, 381*, 315–329.

Redwood, P. S., Lead, J. R., Harrison, R. M., Jones, I. P., & Stoll, S. (2005). Characterization of humic substances by environmental scanning electron microscopy. *Environmental Science and Technology, 39*, 1962–1966.

Séquaris, J. M., & Lewandowski, H. (2003). Physicochemical characterization of potential colloids from agricultural topsoils. *Colloids and Surfaces A: Physicochemical and Engineering Aspects, 217*, 93–99.

Stordal, M. C., Santschi, P. H., & Gill, G. A. (1996). Colloidal pumping: Evidence for the coagulation process using natural colloids tagged with ^{203}Hg. *Environmental Science and Technology, 30*, 3335–3340.

Xiong, Y. (1985). *Soil colloids (I) research methods for soil colloids*. Beijing: Science Press.

Wen, L. S., Santschi, P., Gill, G., & Paternostro, C. (1999). Estuarine trace metal distributions in Galveston Bay: Importance of colloidal forms in the speciation of the dissolved phase. *Marine Chemistry, 63*, 185–212.

Whitesides, G. M., & Grzybowski, B. (2002). Self-assembly at all scales. *Science, 295*, 2418–2421.

Wilding, A., Liu, R. X., & Zhou, J. L. (2004). Validation of cross-flow ultrafiltration for sampling of colloidal particles from aquatic systems. *Journal of Colloid and Interface Science, 280*, 102–112.

Wilkinson, K. J., Balnois, E., Leppard, G. G., & Buffle, J. (1999). Characteristic features of the major components of freshwater colloidal organic matter revealed by transmission electron and atomic force microscopy. *Colloids and Surfaces A: Physicochemical and Engineering Aspects, 155*, 287–310.

Zhou, X. L., & Wangersky, P. J. (1989). Study of copper-complexing organic ligands: Isolation by a Sep-Pak C18 column extraction technique and characterization by Chromarod thin-layer chromatography. *Marine Chemistry, 26*, 21–40.